ASTRONOMY & ASTROPHYSICS
SUPPLEMENT SERIES

Astron. Astrophys. Suppl. Ser. **55**, 411-424 (1984)

Photoelectric photometry of the peculiar emission-line star GG Carinae (*)

E. Gosset, J. Surdej (**) and J.-P. Swings

Institut d'Astrophysique, Université de Liège, avenue de Cointe, 5, B-4200 Cointe-Ougrée, Belgium

Received July 22, accepted October 27, 1983

Summary. — The first extensive sets of photoelectric observations of the peculiar emission-line star GG Carinae were obtained from 1977 to 1981, in both the standard *UBV* and Strömgren systems. A Fourier analysis of 767 independent measurements leads to the determination of a period $P = 31^{d}.020$ for the light variations. Different physical arguments based on the analysis of the present photoelectric — as well as previous photographic — data clearly indicate, however, that the true period is $P = 62^{d}.039$. The resulting composite lightcurve displays two distinct maxima and minima with a total light amplitude $\Delta m \sim 0.5$ mag. Additional interesting features are noticed in the mean lightcurve. Although it is not possible to classify GG Carinae among any known type of variable stars, the light variations of this object are similar to those observed for β Lyrae-type systems. Other possible periodicities as well as the large observed scatter of the photometric data do not preclude that at least one of the two hypothetical components be an intrinsic variable. Noticeable color variations during one full cycle of light variations are also described.

Key words : GG Carinae — photometry — emission-line stars — eclipsing binaries.

1. Introduction.

At the end of the 19th century, GG Carinae ([1]) was already known to be a peculiar star showing a spectrum with bright emission-lines (Pickering, 1896a, b ; Cannon, 1915). Spectroscopic observations by Smith (1955) and Carlson and Henize (1979) suggested that GG Carinae was a Bep-type star. Actually, GG Carinae appears as a Bep and/or a P Cygni type object, depending on the dispersion used when recording its spectrum. Higher resolution data definitely reveal a P Cygni line profile at Hγ as well as many emission lines of both [Fe II] and Fe II, the latter being resolved in two emission components (Swings, 1974).

Hernandez *et al.* (1981) gave a period of 31.03 days for GG Carinae on the basis of radial velocity measurements of different H absorption components. Due, however, to the very heterogeneous set of spectrograms on which their study is based as well as their *a priori* knowledge of a period for the light variability, their result appears very unconvincing (see their radial velocity curve).

Kruytbosch (1930) was the first to investigate the light variability of GG Carinae. He estimated the brightness of this star on the basis of 805 plates taken with the Franklin-Adams instrument at Johannesburg. From the 13 most pronounced minima (five of which come from older observations) displayed in the lightcurve, he derived a period $P = 31^{d}.043 \pm 0^{d}.014$ with a total light amplitude $\Delta m \sim 0.5$ mag. Kruytbosch emphasized that the light variability of GG Carinae might be due to a star « which is at the same time an eclipsing system and a genuine variable ». In a search for variable light in stars having P Cygni type spectra, Hoffleit (1933) concludes that GG Carinae is an eclipsing binary with a period twice as long as that reported by Kruytbosch. Unfortunately, no clear argumentation is presented in favour of such a model. In another investigation, Greenstein (1938) combined 595 photographic observations to construct a mean lightcurve of GG Carinae. She also derived a period $P = 62^{d}.07$, although some variability is present between individual cycles. She concluded that « if GG Carinae is an eclipsing system, there is no doubt that one, or, more probably both, components are variable ». GG Carinae has also been observed by Gaposchkin (1953) during his survey of variable stars (1938-1947). Adopting a period $P = 62^{d}.086$, i.e. twice the period published by Kruytbosch (1930), he reproduces the composite lightcurve of GG Carinae without giving any further detail. As our paper was ready to be submitted, we became aware of recent *UBVRI* photometric observations of the same object by Chen *et al.* (1983). Although their data only cover a small part of the period of the light variation observed for GG Carinae, we nevertheless decided to take them into account : they will be referred hereafter to as CKA

(*) Based on observations collected at the European Southern Observatory, La Silla (Chile).

(**) Also, Chercheur qualifié au Fonds National de la Recherche Scientifique (Belgium), presently at the European Southern Observatory, Garching (FRG).

Send offprint requests to : E. Gosset.

([1]) = CPD-59°2855 = CD-59°3425 = HD 94878 = MWC 215 = Wra 691 = He 3-526.

and discussed in section 3.6. To our knowledge, no further optical photometric observations of GG Carinae have been reported in the literature. Let us still mention however that Allen (1973) and Hagen (1979) find GG Carinae to have an infrared excess of the type believed to originate in a circumstellar dust shell (see also Allen and Swings, 1976 ; Bouchet and Swings, 1982).

The aim of this paper is to present and analyze the first extensive sets of photoelectric observations of GG Carinae. These measurements have been carried out with the Danish 50 cm, ESO 50 cm, Bochum 61 cm and ESO 1 m telescopes in the *UBV* and Strömgren photometric systems at the European Southern Observatory (La Silla, Chile) during the period 1977-1981. The techniques of observation and reduction, the determination of the photometric period as well as a discussion of the results are presented in the next sections.

2. Observations.

During the period 1977-1981, several campaigns of photometric — and occasionally spectroscopic — observations of GG Carinae have been organized at the European Southern Observatory using various telescopes. It should be noted here that a major fraction of the photometry was performed by M. Klutz. We describe hereafter the observation and reduction techniques of the photometric data in both the *UBV* and Strömgren systems.

2.1 *UBV* PHOTOMETRY. — During the months of February, March, 1978 and February, March, 1979 (resp. February, 1977 and April, 1978) *UBV* photoelectric observations of GG Carinae have been carried out with a single channel photometer attached to the Cassegrain focus of the ESO 50 cm and/or 1 m (resp. Bochum 61 cm) telescopes. During each run, the photometer was equipped with an EMI 6256 photomultiplier, Schott standard filters and a Peltier (resp. dry ice) cooling system. A basic integration time of ~ 40 s was chosen when collecting the photons within a ~ 20 arcsec diaphragm. The measurements with both the ESO 50 cm and 1 m telescopes were performed in the pulse counting mode ; while working with the Bochum 61 cm telescope, the data acquisition was performed with an electronic integrating amplifier whose output is recorded on a Philips model PM 8000 potentiometric recorder.

The general observing routine included frequent measurements of GG Carinae, sky, comparison stars and some E region standard stars (Cousins and Stoy, 1962). During the first observing campaign, four comparison stars C1, C2, C3 and C4, chosen for their proximity to GG Carinae and similarity in brightness (see Table I), were regularly measured. C1 (V = 9.33, B-V = 1.73, U-B = 2.06 mag) and C4 (V = 8.98 :, B-V = 1.79 :, U-B = 1.99 : mag) were found to be both very red objects with colors typical of M-type stars. Within a week, C4 appeared to be slightly variable ($\Delta V \sim 0.05$ mag). Between March 31 and April 3, 1978, C3 (V = 9.10 :, B-V = 0.13, U-B = − 0.74 mag) was also found to display light variations as large as 0.09 mag in all three bands. Due to the colors observed for GG Carinae (see below) and considering the previous remarks, we have finally decided to adopt C2 (V = 9.327, B-V = 0.035, U-B = − 0.366 mag) as the best comparison star for GG Carinae and to use C1 as a check comparison star.

After reducing the photometric data to the standard *UBV* system in the usual way, i.e., taking into account the first and second order extinction as well as a linear color transformation, we have estimated for the comparison star C2 that the mean standard deviations were on the average 0.020, 0.010 and 0.010 mag in V, B-V and U-B, respectively. Magnitudes in V as well as B-V and U-B color indices for GG Carinae are listed in table IIA together with the epoch of observation (J. D.).

2.2 STRÖMGREN PHOTOMETRY. — *uvby* photoelectric observations of GG Carinae have been regularly carried out during the months of January, February in 1979 and 1980 (resp. January, 1980) with the Bochum 61 cm (resp. Danish 50 cm) telescopes. During 1979, 1980 and 1981, additional observations have also been obtained by Ardeberg with the Danish 50 cm, Bochum 61 cm and ESO 1 m telescopes. When observing with the Bochum 61 cm and ESO 1 m telescopes, a single channel photometer similar to that described in section 2.1 was used with an EMI 9502 A photomultiplier and u, v, b, y ESO standard filters (see ESO Users Manual, 1982). The Danish 50 cm telescope was equipped with the four-channel Danish photometer which measures simultaneously the light in all four Strömgren bands (see Grønbech *et al.*, 1976, for a description of the photometer and of the pulse counting data acquisition system).

With the only exception of the observations performed by Ardeberg, extinction corrections derived from measurements of the comparison star C2 at different airmasses were applied to the data and instrumental magnitude differences between GG Carinae and C2 calculated. Mean extinction coefficients were used for reducing the observations of Ardeberg. Except for a few measurements he obtained with the Danish 50 cm telescope between December 5 and 25, 1979, the agreement between his and other overlapping observations of GG Carinae is found to be essentially good. We are, however, aware that instrumental problems occurred during December, 1979 with the four-channel Danish photometer (Ardeberg, 1982). Magnitudes in y, b, v and u for GG Carinae are listed in table IIB together with the epoch of observation (J. D.).

During a few good photometric nights, some standard stars were also observed and the data transformed into the standard system. The method of reduction was basically that described in Crawford and Barnes (1970). The magnitude and Strömgren indices of the comparison star C2 were derived as : y = 9.332, b-y = 0.055, m_1 = 0.073 and c_1 = 0.719 mag with typical standard deviations of 0.016, 0.012, 0.022 and 0.046 mag, respectively.

3. Period determination.

An examination of the photometric data compiled in table II clearly shows that GG Carinae displays large light variations ($\Delta m \sim 0.5$ mag in the y and V bands) with well defined maxima and minima. A typical time

interval between two successive similar extrema is about 30 days. However, there seems to be a systematic difference between the brightness of two consecutive maxima ($\Delta m \sim 0.05$ mag). Further arguments will be subsequently presented in favour of a ~ 60-day period for the light variability of GG Carinae.

Since the photometric observations recorded around January 19, 1980 show a well shaped minimum, we decided to accurately determine the epoch of this minimum in order to compute the ephemeris and phases of the lightcurve of GG Carinae. Fitting 2nd and 3rd degree polynomials by a least squares method, we have indicated in table III the epoch as well as the mean standard deviation affecting the determination of that minimum as recorded in the *y*, *b* and *v* bands. The minimum in the *u* band is somewhat flat-bottomed and was therefore not used to derive an epoch.

We made a Fourier analysis of the data published by Kruytbosch (1930) and of those listed in table II. The first step in this procedure consisted in evaluating the power spectrum. For this purpose, we used the DFT (Discrete Fourier Transform) algorithm described by Deeming (1975) as well as the slightly different approach given by Ponman (1981). Both methods appear very suitable when analyzing unequally spaced data, mainly when gaps exist between different groups of data.

3.1 FOURIER ANALYSIS OF KRUYTBOSCH'S DATA. — In his pioneering work, Kruytbosch (1930) lists the mean photographic magnitudes of GG Carinae observed during 249 nights. Although his measurements are not exactly equally spaced in time, we can estimate a critical frequency — i.e. the analog of Nyquist frequency — to be $\nu_c \sim 0.5$ day^{-1}. Therefore, we have calculated the power spectrum of his data in the frequency interval [0.0, 0.5] day^{-1}. After removing the mean value of the 249 mean photographic magnitudes, the calculated power spectrum appears as shown in figure 1. Following Deeming (1975), the square of the full amplitude of the spectral window is given for comparison in figure 1a ; figure 1b represents the square of the full amplitude of the DFT. Figure 1c shows the SE (Spectral Estimate) for the data $P(\nu)$ as defined by Ponman (1981). Figure 1d illustrates the spectral estimate $P_G(\nu)$ for a pure sine monochromatic wave sampled in exactly the same way as were the photometric observations of GG Carinae. The frequency of the pure sine monochromatic wave is always that derived for the star from parts b and c of the same figure. In each of these figures, the ordinate refers to the square of the full amplitude, expressed in (mag)^2, after normalization to unity.

The spectral window (Fig. 1a) is undoubtedly nicely shaped. The width of the main peak is inversely proportional to the time interval covering the analysed set of observations. A first satellite peak — having less than half (50 %) the power of the main peak — at $\nu \sim 0.003$ day^{-1} accounts for the annual periodicity of the observations. A second satellite peak (~ 9 %), at $\nu \sim 0.034$ day^{-1} corresponds to the lunar synodic month. Finally, a third satellite peak (~ 3 %) at $\nu \sim 0.070$ day^{-1} stands for the mean duration of consecutive observations within a month.

The DFT in figure 1b displays an outstanding peak at $\nu \sim 0.032$ day^{-1}. The main characteristics of this peak are summarized in table IV. Let us notice the very similar appearance between the DFT in figure 1b and the SE in figure 1c. Comparison between figures 1b, 1c and 1d is useful in order to distinguish between those remaining peaks in the power spectrum which are due to the noise background and/or to the way the observations were performed (sampling in time).

Finally, we have applied the PDM (Phase Dispersion Minimization) method of Stellingwerf (1978) to the data of Kruytbosch. The relative error between the periods derived by the DFT and PDM methods does not exceed 10^{-5}, a result which is found to be quite satisfactory owing to the high noise background affecting the original data.

Due to the very different methods used when determining a photometric period for GG Carinae, it is in fact quite surprising to notice that the period $P = 31^d.043$ reported by Kruytbosch in 1930 is in such a good agreement with the one derived here ($P = 31^d.051$).

3.2 FOURIER ANALYSIS OF THE *y* AND *V* PHOTOELECTRIC DATA LISTED IN TABLE II. — Taking advantage of the good agreement between the *y* and *V* magnitudes measured for the comparison star C2 (see Sect. 2), we applied a Fourier analysis to the 767 *y* and/or *V* magnitudes of GG Carinae listed in table II. The results of this analysis are illustrated in figure 2.

The time interval covering our observations was shorter than that of Kruytbosch ; it is therefore natural to observe a larger width for the main peak of the spectral window (see Fig. 2a). The numerous satellite peaks which are found on both sides of the main peak — within $\Delta\nu \sim 0.017$ day^{-1} — directly arise from the fact that the maximum time interval of consecutive observations carried out within a single campaign never exceeds sixty days. The DFT in figure 2b as well as the SE in figure 2c still display an outstanding peak at $\nu \sim 0.032$ day^{-1} (see Table IV). There is essentially a good agreement between the period derived here and that determined in section 3.1.

It is interesting to notice from figure 2d that most of the peaks appearing in figures 2b and 2c are inherent to the distribution in time of our photoelectric observations. Furthermore, one readily sees that the noise background affecting the power spectra in figure 2 is much smaller than that in figure 1. Let us further remark that no harmonics are visible in the power spectrum : this situation will clearly lead to a smooth lightcurve.

3.3 THE COMPOSITE LIGHTCURVES OF GG CARINAE. — After removing some uncertain photoelectric measurements recorded between December 5 and 25, 1979 (cf. Sect. 2.2), we have illustrated in figures 3 and 4 the mean composite (*y*/*V*) lightcurves of GG Carinae assuming $P = 31^d.020$ and $P = 62^d.039$, respectively. The trend of light variations appears to be rather smooth. However, the mean scatter of the observations is found to be abnormally high for the lightcurve illustrated in figure 3 when compared to that in figure 4. In fact, the mean scatter derived from figure 4 is about that expected on the basis of the mean scatter observed for the

comparison star C2. We develop hereafter three arguments which give further support to the 62-day period.

i) As mentioned before, there seems to be a systematic difference ($\Delta m \sim 0.05$ mag) between the brightness levels of two consecutive maxima (see Fig. 4). Nevertheless, it should be kept in mind that, with the exception of Ardeberg's data (Δ and ∇ symbols), the two maxima were not homogeneously covered since the observations were performed with different instruments.

Let us now define a nomenclature for the different extrema : in the following, the minimum for which we have derived an epoch in table III will be referred to as Min I ($\phi = 0.0$ in Fig. 4) ; it is then followed by the brightest (Max I) of the two maxima and subsequently by Min II and Max II. Since the two minima recorded in the lightcurve of GG Carinae have approximately the same depth, it is not possible to distinguish between the primary and/or secondary minimum.

ii) The mean composite lightcurve of GG Carinae illustrated in figure 4 is definitely asymmetric. Max I appears sharper than Max II, the slopes on both sides of these two maxima being also quite different. Furthermore, Min II occurs well before half the period value, i.e. at phase $\phi = 0.44$. This constitutes the most significant fact that leads us to adopt the 62-day period.

We have also looked for the presence of such lightcurve asymmetries in Kruytbosch's data. Due to the large scatter affecting his observations, we have used a sliding-unweighted-mean in order to construct the relevant composite lightcurve of GG Carinae. Adopting $\Delta\phi = 0.090$ for the window size and $P = 62^{\mathrm{d}}.102$ for the period, we have illustrated in figure 5 the results of these calculations where the reported lightcurve asymmetries as well as the phase shift of Min II are clearly present.

iii) At phase $\phi = 0.23$, i.e. just before Max I, there appears to be a sudden decrease ($\Delta m \sim 0.1$ mag) in brightness of GG Carinae, lasting slightly more than one day. There is no doubt about the reality of this observation. Indeed, it was simultaneously observed on February 3, 1980 with the Bochum 61 cm telescope (+ symbols in Fig. 4) and with the Danish 50 cm telescope (Δ symbols in Fig. 4). On August 8, 1980 ($\phi \sim 0.23$), this sudden decrease in brightness (hereafter referred to as Min III) was again observed with the Danish 50 cm telescope (∇ symbols). In the framework of a binary star model, there is no obvious explanation for such an observation. Additional photoelectric measurements are highly desirable in order to firmly establish the persistence of this Min III.

Applying again the sliding mean technique — with a window size $\Delta\phi \lesssim 0.04$ — to Kruytbosch's data, we find some good evidence for the presence of this Min III.

3.4 More on the period determination. — Let us first remark that because the Fourier transform is nothing more than a fit of sine and cosine wave-functions to a given set of data, the resulting period determination will consequently remain insensitive to the presence of small scale features such as those discussed above (e.g. Min III).

On the other hand, adopting a period that is twice the value derived from the Fourier analysis in section 3.2 consists in a rather crude method which requires an *a posteriori* confirmation. Indeed, since the composite lightcurve of GG Carinae displays two asymmetric maxima and minima, one easily predicts that there will be an over — or under — estimate of the half period value depending on the observed distribution of the data points over the four extrema. Different weights were thus given to the data, depending on their phase location. For given sets of arbitrary weighting factors, we then computed the relevant periods following a similar procedure as before. The results appear fairly insensitive to the assumed distributions.

We have applied once more the PDM method (Stellingwerf, 1978) to the set of photoelectric observations compiled in table II. The Θ_s statistics presents two clear minima at the frequencies $\nu \sim 0.032$ and $\nu \sim 0.016$ day^{-1}. However, on the only basis of statistical arguments, it is not possible to decide which of these two minima is the most significant one, i.e. which period is the most plausible one. In fact, in his statistical analysis, Stellingwerf makes implicit assumptions that are generally not fulfilled (see Horman, 1980). One of these namely relies on the fact that the data population has almost the same variance in each phase-bin. This assumption is of course in contradiction with the general variation of our photoelectric data (see above).

Let us finally describe the method that we have used in order to derive the best period value as well as its uncertainty. Using a non-linear least squares method, we have fitted our data in table II with a Fourier expansion up to the 3 θ terms. Leaving the frequency ν as a free parameter, the best fit determination leads to :

$$\nu = 0.016119 \text{ with } \sigma_\nu = 0.000016 \text{ day}^{-1},$$
$$\text{i.e. } P = 62^{\mathrm{d}}.039 \text{ with } \sigma_P = 0^{\mathrm{d}}.060 .$$

3.5 Search for other periodicities. — Following the suggestions by Kruytbosch (1930) and Greenstein (1938) that GG Carinae is possibly a binary system with — at least — one of the components being a genuine variable, we searched through our photoelectric data for the presence of other periodicities. *Via* an iterative process, we first whitened the y and V photometric observations by subtracting the variations due to the main frequency component until the standard deviation around the mean level became constant. Next, we applied again the DFT and SE methods. The relevant power spectra were computed in the frequency interval $\nu \in [0.0, 1.5]$ day^{-1}. Many peaks can be seen, the principal ones being located at $\nu \sim 0.045$, 0.3657, 0.6356, 0.955, 1.045 and 1.3657 day^{-1}. It is easy to show that these peaks can be separated in two distinct families, the peaks within a same family being aliases of one another. The first family includes the peaks at $\nu \sim 0.045$, 0.955 and 1.045 day^{-1}, the most important one at $\nu \sim 1.045$ day^{-1} being the most probable genitor of this family. However, this family is found to present a peculiar behaviour. Indeed, the heights of these peaks are directly proportional to the residuals of the whitening iterative process. It is therefore concluded that this first family is nothing more than an artefact of the bad whitening of the data when subtracting the variations due to the main frequency component.

Consequently, in order to remove the effects of the lightcurve asymmetries, we whitened once more our data with a Fourier expansion up to the 3 θ terms for the 31- and 62-day periods. We then iterated several times to ensure the reliability of the whitening process. The power spectrum of the result is shown in figure 6 where an arbitrary unit along the ordinate typically represents one mean standard deviation (1 σ). The pattern of the spectral window in figure 6a is of course the same as that in figure 2a. The main pattern is recurrent near $\nu = 1.0$ day^{-1}, confirming the value $\nu_c \sim 0.5$ day^{-1} for our data. In figures 6b and c, the power spectrum displays a complex structure : the heights of the principal peaks are comparable to one mean standard deviation and the noise background appears consequently well resolved. Among the numerous peaks visible in those figures, only three reproduce fairly well the pattern of the spectral window. These are the peaks located at $\nu \sim 0.3657$, 0.6356 and 1.3657 day^{-1}, which are the members of the second family. The peaks of the first family are now almost entirely removed. All other remaining peaks have no statistical significance : they are formed by the random superposition of the noise and aliases of other peaks. In figure 6d, we have reproduced the two spectral estimates $P_G(\nu)$ for a pure sine wave-function corresponding to the low frequency peak at $\nu \sim 0.3657$ day^{-1} (continuous line) and to the peak at $\nu \sim 0.6356$ day^{-1} (dotted line). As the heights of these different peaks do not differ significantly, it is not easy to derive which one is the real genitor. However (see Figs. 6b-d), the peak at $\nu \sim 0.6356$ day^{-1} seems to be the most likely candidate.

Although data redistributed in a phase diagram with the above periods to not show a clear trend of light variations (except perhaps some small variations for $\nu \sim 0.3657$ day^{-1}), this does not constitute a valid argument against the existence of the claimed periodicities. Indeed, the Fourier techniques can detect periodicities that are far under the noise level. Let us also remark the possibility that such peaks arise from oscillations that are stable in frequency but of random distributed phases and with unstable amplitudes such as those observed in the V filter near phase $\phi = 0.7$.

Finally, we have also applied a Fourier analysis to the absolute photometric data of the comparison star C2. There is no evidence for the presence of any periodicity. We therefore conclude that the small scale light variations detected in the lightcurve of GG Carinae are very likely to be real (probability ~ 85 %, i.e. a significance level of ~ 0.15). The most probable frequency of these light variations is found to be $\nu \sim 0.6356$ day^{-1} corresponding to $P \sim 1.6$ day — although the frequency $\nu \sim 0.3657$ day^{-1} — corresponding to $P \sim 2.7$ days — cannot be totally rejected. It should be noted that higher frequencies aliases of those values cannot be rejected either. An extensive set of continuous photometric observations of GG Carinae would be very suitable in order to confirm these small scale light variations.

3.6 THE CKA DATA. — Combining our y and V measurements with those of CKA, we tried to derive a global period for the light variations of GG Carinae. Chen *et al.* (1983) observed GG Carinae simultaneously with two comparison stars which turned out to be our C2 and C3 ; the magnitudes they give for C3 confirm, at least within a smaller range, the variability that we report for this star (see Sect. 2.1).

On the basis of our ephemeris, it appears that CKA observed for GG Carinae an ingress towards Min II at Mount Johnson and an egress from Min I at Cerro Tololo : without any clear argumentation, CKA name these minima as being the « primary » and « secondary » ones, respectively. We then computed the GG-C2 data for each night and performed a Fourier analysis of both their V and our y and V data. From this analysis, we find that an outstanding peak is present at $\nu \sim 0.032$ day^{-1} : its main characteristics are summarized in table IV. The resulting period is found to be in better agreement with that calculated from Kruytbosch's data. However, if one redistributes the relevant data in a phase diagram with either the 62.039 or 62.082 day period, it is clearly seen that :

i) the Mount Johnson data are fairly well located in the descending branch towards Min II ;

ii) there is a rather poor overlap between the Cerro Tololo data and ours.

In fact, the first photoelectric observations carried out at Cerro Tololo are located near $\phi = 0$ and fit well with Min I. The rise in brightness is then found to be steeper than the one we observed, the CKA measurements reaching, at about $\phi = 0.085$, the two isolated points (∇) that can be seen in figure 4. Afterwards, the CKA data remain constant in brightness in the phase range $\phi \in [0.09, 0.15]$. Therefore, the resulting composite lightcurve resembles that of figure 5, with a « shoulder » at $\phi \sim 0.085$. It is unlikely that such a behaviour could be accounted for by the fact that our data were obtained in the y band while those of CKA were recorded in the V band. Indeed, any variability in the equivalent width of some underlying bright emission lines (Hα, etc.) would then manifest itself differently in the y, V, R or I bands. A look at the CKA data clearly shows that the trend of light variations is nearly the same in the V, R and I bands. Furthermore, since our y measurements are totally insensitive to any of the Balmer lines, we conclude that the departure of the light variations in the ascending branch of Min I is probably due to a peculiar behaviour of the stellar continuum.

4. The lightcurve and color variations of GG Carinae.

Although the photoelectric lightcurve recorded for GG Carinae presents some similarities to those observed from classical close binaries, it is not possible to account for both the observed large amplitude variations ($\Delta m \sim 0.5$ mag) and the derived long period ($P = 62^d.039$) by the only ellipsoidality of the two hypothetical components. Therefore, it is likely that GG Carinae is an eclipsing binary system. The absence of signs of ingress or egress due to eclipses seems to be reminiscent of the lightcurve characteristics seen in β Lyrae type systems. The phase shift observed for Min II could then be interpreted as being caused by the eccentricity of the binary orbit. However, the very similar depth observed for the two minima in GG Carinae's lightcurve makes this object

quite distinct from the prototype β Lyrae whose light-curve displays two very different minima, with the primary minimum having a depth as great as 1.0 mag (Larsson-Leander, 1969).

Besides the main trend of the light variation observed for GG Carinae (see Fig. 4), smaller scale variabilities are also present, as already discussed in section 3.5. Furthermore, extensive observations carried out during a few single nights with the Geneva 70 cm telescope at La Silla (Bartholdi, 1983) show a scatter in the photometric measurements that can only be attributed to intrinsic variations of GG Carinae. It therefore seems to be well established that at least one of the two components of the system is a rapidly variable star (cf. Hoffleit, 1933 ; Greenstein, 1938).

As far as the color indices are concerned, GG Carinae is found to present a similar behaviour in the v and b bands, the average v-b color index for GG Carinae being + 0.343 mag (σ = 0.018 mag). It is likely that one or both of the following effects play a role : Hδ, which « contaminates » the v pass band contributes negligibly, with respect to the stellar continuum, to the v measurements, and/or the complex Balmer lines vary in parallel with the underlying continuum. The observed variations in the y band are found to be slightly smaller than those seen in the two previous channels. Figure 7 illustrates the behaviour of the b-y color index for GG Car : whereas no obvious color differences are detected between the two minima (ϕ = 0 and ϕ = 0.44), nor between the maxima (ϕ = 0.25 and ϕ = 0.75), the two maxima do appear systematically bluer ($\sim$ 0.05 mag) than the minima. Let us mention that a similar effect is observed in binary systems containing elongated components. Since the v and b magnitudes vary in parallel, the c_1 color index merely reflects relative light variations of GG Carinae between the u and v bands. Figure 8 illustrates the behaviour of y *versus* c_1 for GG Car : a clear correlation is readily seen. Although we have no explanation of this y/c_1 relation, one should be aware that any apparent variation in the physical conditions (integrated effective temperature, etc.) of the system caused by the orbital motion of the components could account for such a correlation. On the other hand, since the light variability of GG Carinae is less pronounced in the u band and since the system is redder at maximum light (i.e. considering c_1), an excess of non-eclipsed ultraviolet radiation (partial filling of the Balmer continuum by emission ?) could be responsible for the observations. Stephenson and Sanduleak (1971) have in fact reported the presence of a Balmer emission continuum in the spectrum of GG Carinae.

If one combines the CKA data with our own measurements, there results a better coverage of the phases during one full cycle of light variations. The B-V color index then appears not to vary by more than 0.05 mag, whereas for the U-B color index, similar conclusions as for c_1 are found to apply. Let us still mention that GG Carinae appears bluer in U-B at Min I than at Min II by as much as 0.06 mag. This is found to be of the same order as for the case of c_1 ($\sim$ 0.09 mag). However, it must be kept in mind that the two minima were not observed with the same instruments.

Finally, we wish to point out that Min III, i.e., the « glitch » observed in Max I, has exactly the same depth in u, v and b, but that it is somewhat less pronounced in y ; no obvious mechanism is however proposed in order to interpret this phenomenon.

5. Intrinsic colors of GG Carinae.

When located in a two-color diagram (e.g., U-B/B-V), GG Carinae appears to be a fairly red object. Nevertheless, the observed U-B color index at maximum light corresponds to that of a normal B3-B5 type star. As mentioned in the previous section, an excess of radiation in the U band could be present. From the spectral characteristics alone (cf. Carlson and Henize, 1979), it is unlikely that GG Carinae could have a E_{U-B} excess greater than 0.35 mag, corresponding to a B0 spectral type. Ultraviolet data obtained with the ANS and IUE satellites also clearly indicate that the hottest component of GG Carinae is not earlier than approximately B0 : these data will be described in a subsequent paper.

If a normal extinction law is used, then an upper limit for E_{B-V} is found to be of the order of 0.5 mag. Therefore, an intrinsic $(B-V)_0 \sim 0.0$ mag is derived, corresponding to a late B or more probably to an early A type star. Similar conclusions are drawn on the basis of the available Strömgren photometry. A cool component could thus possibly be detected in the binary system from red and/or near-infrared photometry. Such observations were performed by CKA. However, considering the physical parameters derived by these authors, it is surprising to note that no spectral feature of a cool component has ever been detected (e.g. Carlson and Henize, 1979). It is safe to conclude that GG Carinae reveals itself as being a quite unusual system and that no « such a simple model » as that suggested by CKA can account for the main observed characteristics of GG Carinae.

6. Concluding remarks.

This paper presents the first period determination of the light variability of GG Carinae on the basis of extensive sets of photoelectric photometry, and a strong argumentation has been developed in favor of a 62-day period. The composite lightcurve of GG Carinae is essentially smooth during one full cycle. Color variations have also been reported. At this stage, it is tempting to classify GG Carinae as a possible candidate of β Lyrae type systems. The minima observed in the lightcurve appear to be very similar, whereas the two maxima exhibit slight differences. A phase shift exists for the second minimum and it probably reflects the eccentricity of the orbit. An additional minimum (Min III) has been detected on the brightest maximum (Max I) but there is no obvious explanation for its presence. A secondary period (1.6 and/or 2.7 days) has been found in the Fourier analysis at a 0.15 significance level, suggesting that at least one of the components is a genuine variable (cf. Hoffleit, 1933).

GG Carinae has now been kindly included for systematic monitoring in the Geneva photometric system : it will therefore be regularly observed with the Geneva 70 cm telescope at La Silla (Chile), and this will eliminate the inhomogeneity problems that were affecting our data.

In order to define the orbital elements, the energy distribution, etc. of the GG Carinae system, we have now begun to analyze several tens of coudé spectrograms (12 and 20 Å mm^{-1}) that are at our disposal as well as IUE data. This work is in progress and the results will be presented in a subsequent paper.

Acknowledgements.

The analysis presented here relies on observations performed essentially by A. Ardeberg, M. Klutz and H. Lindgren to whom we express our sincere thanks ; additional data were also kindly provided by G. Adam, P. Bouchet, J. Manfroid, P. Mianes and N. Vogt.

One of us (E.G) is particularly indebted to P. Bartholdi for his hospitality and great help during a visit to Geneva and to J. Manfroid for help and fruitful discussion concerning the PDM method. The same author further thanks the « Fonds de la Recherche Fondamentale Collective » for financial support (contrat n° 2.9002.76).

References

ALLEN, D. A. : 1973, *Mon. Not. R. Astron. Soc.* **161,** 145.
ALLEN, D. A., SWINGS, J. P. : 1976, *Astron. Astrophys.* **47,** 293.
ARDEBERG, A. : 1982, private communication.
BARTHOLDI, P. : 1983, private communication.
BOUCHET, P., SWINGS, J. P. : 1982, *IAU Symp.* N° 98 « Be Stars », eds. Jaschek M. & Groth H. G., p. 241.
CANNON, A. J. : 1915, *Harvard Ann.* **76,** 31.
CARLSON, E. D., HENIZE, K. G. : 1979, *Vistas Astron.* **23,** 213.
CHEN, K. Y., KOWALSKE, K., AUSTIN, R. R. D. : 1983, *Publ. Astron. Soc. Pac.* **95,** 157.
COUSINS, A. W. J., STOY, R. H. : 1962, *R. Obs. Greenwich-Cape Bull.* N° 49, 58S.
CRAWFORD, D. L., BARNES, J. V. : 1970, *Astron. J.* **75,** 978.
DEEMING, T. J. : 1975, *Astrophys. Space Sci.* **36,** 137.
GAPOSCHKIN, S. : 1953, *Harvard Ann.* **113,** N° 2.
GREENSTEIN, N. K. : 1938, *Harvard Bull.* **908,** 25.
GRØNBECH, B., OLSEN, E. H., STRÖMGREN, B. : 1976, *Astron. Astrophys. Suppl. Ser.* **26,** 155.
HAGEN, W. : 1979, *Astron. J.* **84,** 1189.
HERNANDEZ, C. A., LOPEZ, L., SAHADE, J., THACKERAY, A. D. : 1981, *Publ. Astron. Soc. Pac.* **93,** 747.
HOFFLEIT, D. : 1933, *Harvard Bull.* **892,** 19.
HORMAN, M. : 1980, unpublished Thesis, Univ. de Liège, Chap. IV.
KRUYTBOSCH, W. E. : 1930, *Bull. Astron. Inst. Netherl.* **6,** 11.
LARSSON-LEANDER, G. : 1969, *Arkiv Astron.* **5,** N° 17.
PICKERING, E. C. : 1896a, *Astron. Nachr.* **141,** 169.
PICKERING, E. C. : 1896b, *Harvard Circ.,* N° 9 (also *Astrophys. J.* **4,** 142).
PONMAN, T. : 1981, *Mon. Not. R. Astron. Soc.* **196,** 583.
SMITH, H. J. : 1955, *Southern Wolf-Rayet Stars* ; Ph. D. dissert., Harvard Univ.
STELLINGWERF, R. F. : 1978, *Astrophys. J.* **224,** 953.
STEPHENSON, C. B., SANDULEAK, N. : 1971, *Publ. Warner & Swasey Obs.* - Case Western Reserve Univ., Vol. I, N° 1.
SWINGS, J. P. : 1974, *Astron. Astrophys.* **34,** 333.

TABLE I. — *Spectral type, photographic magnitude (cf. SAO & Cape Catalogs) and equatorial coordinates of GG Carinae and selected comparison stars.*

Identification	CPD number	Sp. type	m_{ph}	α(1950.0)	δ(1950.0)
GG Carinae	-59°2855	pec.	8.7	$10^h53^m58^s$	-60°07'31"
C1	-59°2861	-	9.8	10 54 18	-60 10 48
C2	-59°2873	B 8	9.2	10 55 04	-60 11 18
C3	-59°2856	B 3	9.0	10 54 03	-60 13 35
C4	-59°2857	-	9.6	10 54	-60 07 06

TABLE III. — *Epoch (J. D.) of the minimum Min I as recorded in each Strömgren photometric band.*

Filter	y	b	v
Epoch JD : 2440000.+	4259.92	4260.54	4260.18
Standard deviation σ	0.40	0.32	0.33

TABLE IV. — *Characteristics of the main peaks in Fig. 1 and Fig. 2.*

	Position		Half width at half maximum		Numerical resolution	
	$\nu(day^{-1})$	P(day)	$\nu(day^{-1})$	P(day)	$\nu(day^{-1})$	P(day)
KRUYTBOSCH's data (Fig.1)	0.0322051	31.0509	$6.0\ 10^{-5}$	$5.8\ 10^{-2}$	$4.0\ 10^{-7}$	$4.0\ 10^{-4}$
Our y,V data (Fig.2)	0.0322376	31.0197	$4.0\ 10^{-4}$	$4.0\ 10^{-1}$	$4.0\ 10^{-7}$	$4.0\ 10^{-4}$
Our y,V data + those of CKA	0.0322155	31.0410	$4.0\ 10^{-4}$	$4.0\ 10^{-1}$	$4.0\ 10^{-7}$	$4.0\ 10^{-4}$

TABLE IIA. — *Epochs and photometric data for GG Carinae in the Johnson system (see text).*

JD. 2440000.+	V	B-V	U-B	INSTRUMENT	JD. 2440000.+	V	B-V	U-B	INSTRUMENT
3562.63	8.570	0.568	-0.642	UBV	3599.73	8.782	0.580	-0.738	UBV
3562.64	8.572	0.570	-0.647	UBV	3599.74	8.777	0.591	-0.749	UBV
3563.64	8.581	0.57:	-0.636	UBV	3601.70	8.771	0.572	-0.819	UBV
3563.64	8.589	0.559	-0.639	UBV	3602.68	8.827	0.589	-0.846	UBV
3570.68	8.838	0.600	-0.817	UBV	3602.69	8.839	0.593	-0.836	UBV
3570.68	8.843	0.603	-0.826	UBV	3603.67	8.837	0.575	-0.881	UBV
3571.67	8.870	0.598	-0.818	UBV	3603.67	8.826	0.587	-0.869	UBV
3571.67	8.873	0.601	-0.825	UBV	3604.69	8.875	0.573	-0.865	UBV
3572.67	8.912	0.598	-0.848	UBV	3604.70	8.875	0.581	-0.860	UBV
3572.67	8.906	0.603	-0.842	UBV	3604.72	8.868	0.575	-0.859	UBV
3573.68	8.860	0.592	-0.810	UBV	3604.72	8.872	0.573	-0.862	UBV
3573.68	8.867	0.577	-0.803	UBV	3604.72	8.882	0.573	-0.868	UBV
3575.68	8.870	0.595	-0.800	UBV	3604.72	8.882	0.575	-0.870	UBV
3575.68	8.867	0.606	-0.807	UBV	3605.67	8.858	0.564	-0.835	UBV
3596.61	8.667	0.592	-0.742	UBV	3605.68	8.863	0.564	-0.838	UBV
3596.61	8.662	0.598	-0.744	UBV	3605.69	8.862	0.559	-0.843	UBV
3596.71	8.650	0.593	-0.763	UBV	3605.69	8.865	0.563	-0.831	UBV
3596.72	8.658	0.583	-0.744	UBV	3605.71	8.860	0.567	-0.860	UBV
3596.73	8.662	0.581	-0.751	UBV	3605.71	8.856	0.566	-0.825	UBV
3596.73	8.662	0.582	-0.751	UBV	3605.72	8.866	0.571	-0.835	UBV
3597.63	8.665	0.590	-0.793	UBV	3605.72	8.867	0.568	-0.834	UBV
3597.64	8.660	0.591	-0.793	UBV	3606.53	8.846	0.579	-0.843	UBV
3597.66	8.669	0.585	-0.791	UBV	3606.53	8.861	0.565	-0.859	UBV
3597.66	8.664	0.587	-0.789	UBV	3606.55	8.851	0.561	-0.872	UBV
3597.67	8.662	0.597	-0.793	UBV	3606.55	8.866	0.550	-0.862	UBV
3597.67	8.670	0.586	-0.787	UBV	3606.57	8.844	0.571	-0.873	UBV
3597.69	8.674	0.585	-0.782	UBV	3606.57	8.853	0.577	-0.876	UBV
3597.69	8.683	0.575	-0.785	UBV	3606.59	8.855	0.574	-0.863	UBV
3597.70	8.686	0.575	-0.776	UBV	3606.59	8.866	0.561	-0.866	UBV
3597.71	8.682	0.581	-0.783	UBV	3606.60	8.848	0.572	-0.864	UBV
3597.74	8.690	0.593	-0.786	UBV	3606.60	8.850	0.568	-0.864	UBV
3597.75	8.688	0.590	-0.779	UBV	3607.68	8.862	0.578	-0.852	UBV
3597.77	8.703	0.584	-0.789	UBV	3607.68	8.865	0.582	-0.858	UBV
3597.77	8.709	0.582	-0.783	UBV	3607.69	8.857	0.579	-0.854	UBV
3598.66	8.706	0.600	-0.798	UBV	3607.70	8.856	0.580	-0.853	UBV
3598.66	8.704	0.601	-0.795	UBV	3607.71	8.860	0.577	-0.857	UBV
3598.66	8.708	0.602	-0.805	UBV	3607.71	8.862	0.577	-0.856	UBV
3598.68	8.711	0.595	-0.806	UBV	3607.72	8.859	0.577	-0.852	UBV
3598.68	8.708	0.587	-0.800	UBV	3607.72	8.860	0.587	-0.857	UBV
3598.70	8.714	0.587	-0.802	UBV	3607.73	8.850	0.588	-0.847	UBV
3598.70	8.713	0.583	-0.806	UBV	3607.73	8.850	0.591	-0.843	UBV
3598.73	8.713	0.594	-0.798	UBV	3608.67	8.811	0.553	-0.820	UBV
3598.73	8.717	0.589	-0.797	UBV	3608.67	8.813	0.553	-0.830	UBV
3598.76	8.716	0.597	-0.795	UBV	3608.69	8.823	0.551	-0.834	UBV
3598.76	8.712	0.604	-0.792	UBV	3608.69	8.813	0.560	-0.832	UBV
3599.67	8.784	0.590	-0.743	UBV	3608.70	8.803	0.569	-0.828	UBV
3599.68	8.785	0.586	-0.740	UBV	3608.70	8.802	0.570	-0.827	UBV
3599.69	8.795	0.593	-0.750	UBV	3608.71	8.803	0.570	-0.824	UBV
3599.69	8.786	0.590	-0.761	UBV	3608.72	8.813	0.553	-0.822	UBV
3599.72	8.792	0.582	-0.752	UBV	3608.72	8.869	0.541	-0.787	UBV
3599.72	8.789	0.587	-0.756	UBV	3608.73	8.817	0.561	-0.802	UBV

TABLE IIA *(continued).*

JD. 2440000.+	V	B-V	U-B	INSTRUMENT	JD. 2440000.+	V	B-V	U-B	INSTRUMENT
3609.67	8.793	0.569	-0.847	UBV	3618.65	8.751	0.601	-0.829	UBV
3609.67	8.801	0.566	-0.846	UBV	3618.65	8.751	0.597	-0.824	UBV
3609.68	8.787	0.571	-0.838	UBV	3619.56	8.662	0.613	-0.838	UBV
3609.68	8.782	0.579	-0.836	UBV	3619.56	8.662	0.612	-0.832	UBV
3609.70	8.789	0.569	-0.839	UBV	3619.58	8.654	0.620	-0.828	UBV
3609.70	8.790	0.574	-0.834	UBV	3619.58	8.662	0.610	-0.822	UBV
3609.71	8.779	0.579	-0.843	UBV	3619.59	8.653	0.616	-0.822	UBV
3609.72	8.779	0.578	-0.850	UBV	3619.59	8.663	0.600	-0.827	UBV
3609.72	8.788	0.579	-0.841	UBV	3619.60	8.685	0.609	-0.826	UBV
3609.72	8.787	0.573	-0.843	UBV	3619.60	8.676	0.590	-0.821	UBV
3611.59	8.768	0.599	-0.820	UBV	3621.56	8.656	0.580	-0.749	UBV
3611.59	8.763	0.609	-0.824	UBV	3621.56	8.651	0.579	-0.745	UBV
3611.60	8.770	0.590	-0.819	UBV	3621.58	8.662	0.574	-0.750	UBV
3611.60	8.760	0.599	-0.816	UBV	3621.58	8.661	0.577	-0.744	UBV
3611.62	8.773	0.604	-0.806	UBV	3621.67	8.680	0.570	-0.728	UBV
3611.62	8.772	0.611	-0.807	UBV	3621.68	8.682	0.569	-0.738	UBV
3611.63	8.793	0.621	-0.801	UBV	3621.68	8.683	0.577	-0.728	UBV
3611.63	8.772	0.617	-0.818	UBV	3621.68	8.676	0.567	-0.739	UBV
3612.59	8.798	0.587	-0.787	UBV	3622.59	8.602	0.556	-0.747	UBV
3612.59	8.797	0.592	-0.784	UBV	3622.59	8.594	0.558	-0.741	UBV
3612.60	8.792	0.601	-0.780	UBV	3622.60	8.608	0.543	-0.737	UBV
3612.61	8.793	0.594	-0.786	UBV	3622.60	8.601	0.546	-0.740	UBV
3612.62	8.786	0.603	-0.778	UBV	3622.61	8.610	0.553	-0.741	UBV
3612.62	8.789	0.594	-0.784	UBV	3622.61	8.605	0.547	-0.739	UBV
3612.63	8.789	0.595	-0.779	UBV	3622.62	8.603	0.551	-0.737	UBV
3612.63	8.817	0.573	-0.782	UBV	3622.62	8.602	0.552	-0.746	UBV
3614.57	8.716	0.607	-0.793	UBV	3623.57	8.666	0.547	-0.769	UBV
3614.57	8.716	0.608	-0.798	UBV	3623.57	8.665	0.544	-0.765	UBV
3614.59	8.722	0.597	-0.788	UBV	3623.60	8.653	0.555	-0.768	UBV
3614.59	8.724	0.591	-0.791	UBV	3623.60	8.654	0.550	-0.760	UBV
3614.61	8.723	0.609	-0.781	UBV	3623.61	8.654	0.551	-0.768	UBV
3614.61	8.715	0.604	-0.785	UBV	3623.61	8.650	0.560	-0.770	UBV
3614.62	8.711	0.595	-0.796	UBV	3623.61	8.655	0.557	-0.779	UBV
3614.62	8.712	0.604	-0.794	UBV	3623.61	8.658	0.545	-0.776	UBV
3615.59	8.771	0.608	-0.791	UBV	3623.62	8.660	0.546	-0.770	UBV
3615.59	8.782	0.602	-0.788	UBV	3624.55	8.677	0.574	-0.822	UBV
3615.60	8.779	0.589	-0.799	UBV	3624.55	8.676	0.579	-0.822	UBV
3615.61	8.773	0.595	-0.795	UBV	3624.57	8.677	0.578	-0.822	UBV
3615.62	8.763	0.605	-0.784	UBV	3624.57	8.685	0.570	-0.823	UBV
3615.62	8.758	0.604	-0.802	UBV	3624.59	8.686	0.570	-0.812	UBV
3615.63	8.756	0.608	-0.794	UBV	3624.59	8.681	0.578	-0.812	UBV
3615.63	8.762	0.600	-0.803	UBV	3624.59	8.692	0.572	-0.817	UBV
3616.59	8.720	0.596	-0.837	UBV	3624.60	8.687	0.575	-0.817	UBV
3616.60	8.724	0.596	-0.835	UBV	3625.46	8.701	0.569	-0.836	UBV
3616.61	8.714	0.594	-0.826	UBV	3625.46	8.700	0.572	-0.842	UBV
3616.61	8.713	0.589	-0.814	UBV	3625.47	8.697	0.576	-0.856	UBV
3616.62	8.713	0.593	-0.821	UBV	3625.47	8.696	0.578	-0.854	UBV
3616.62	8.712	0.603	-0.829	UBV	3625.48	8.696	0.586	-0.857	UBV
3616.63	8.709	0.608	-0.821	UBV	3625.49	8.703	0.581	-0.853	UBV
3616.63	8.715	0.598	-0.821	UBV	3625.49	8.700	0.580	-0.851	UBV
3617.61	8.686	0.597	-0.836	UBV	3625.50	8.700	0.586	-0.850	UBV
3617.61	8.678	0.583	-0.829	UBV	3625.50	8.704	0.581	-0.858	UBV
3617.63	8.677	0.591	-0.830	UBV	3177.78	8.832	-	-	UXV
3617.63	8.682	0.592	-0.827	UBV	3178.81	8.796	-	-	UXV
3617.64	8.680	0.594	-0.821	UBV	3179.80	8.768	-	-	UXV
3617.64	8.692	0.575	-0.807	UBV	3180.76	8.731	-	-	UXV
3617.65	8.672	0.593	-0.820	UBV	3181.78	8.770	-	-	UXV
3617.65	8.673	0.583	-0.813	UBV	3182.78	8.685	-	-	UXV
3618.61	8.750	0.607	-0.819	UBV	3183.82	8.676	-	-	UXV
3618.61	8.758	0.602	-0.825	UBV					
3618.63	8.765	0.601	-0.827	UBV					
3618.63	8.766	0.601	-0.824	UBV					
3618.64	8.755	0.606	-0.822	UBV					
3618.65	8.757	0.610	-0.827	UBV					

KEY TO SYMBOLS : UBV (1978-79)
UXV (1977)

TABLE IIB. — *Epochs and photometric data for GG Carinae in the Strömgren system (see text).*

JD. 2440000.+	Y	B	V	U	INSTRUMENT	JD. 2440000.+	Y	B	V	U	INSTRUMENT
4247.64	8.608	9.096	9.448	9.574	MKD	4255.82	8.827	9.343	9.695	9.567	MKD
4247.68	8.646	9.139	9.479	9.566	MKD	4255.82	8.829	9.347	9.702	9.559	MKD
4247.65	8.637	9.095	9.454	9.565	MKD	4255.83	8.840	9.347	9.702	9.552	MKD
4248.64	8.707	9.188	9.518	9.618	MKD	4255.83	8.828	9.338	9.700	9.554	MKD
4248.64	8.712	9.185	9.537	9.636	MKD	4255.83	8.820	9.332	9.699	9.553	MKD
4248.64	8.705	9.183	9.537	9.628	MKD	4255.83	8.813	9.338	9.690	9.559	MKD
4248.65	8.725	9.194	9.558	9.650	MKD	4255.84	8.813	9.348	9.699	9.561	MKD
4248.70	8.702	9.166	9.502	9.638	MKD	4255.84	8.849	9.342	9.681	9.554	MKD
4248.71	8.706	9.178	9.508	9.630	MKD	4255.84	8.825	9.341	9.690	9.557	MKD
4248.72	8.693	9.169	9.506	9.630	MKD	4255.84	8.808	9.338	9.700	9.554	MKD
4248.72	8.694	9.141	9.486	9.628	MKD	4255.84	8.831	9.333	9.697	9.550	MKD
4248.78	8.691	9.160	9.513	9.623	MKD	4255.84	8.823	9.348	9.706	9.566	MKD
4248.79	8.683	9.148	9.504	9.621	MKD	4256.69	8.889	9.403	9.740	9.620	MKD
4248.79	8.688	9.161	9.508	9.622	MKD	4256.69	8.891	9.394	9.748	9.625	MKD
4248.79	8.691	9.154	9.508	9.624	MKD	4256.70	8.894	9.395	9.736	9.639	MKD
4248.80	8.683	9.155	9.509	9.616	MKD	4256.70	8.890	9.409	9.746	9.617	MKD
4248.82	8.678	9.144	9.507	9.607	MKD	4256.70	8.903	9.400	9.755	9.638	MKD
4249.66	8.687	9.190	9.563	9.605	MKD	4256.70	8.902	9.404	9.751	9.633	MKD
4249.71	8.715	9.214	9.571	9.602	MKD	4256.70	8.885	9.400	9.743	9.617	MKD
4249.77	8.714	9.218	9.574	9.592	MKD	4256.71	8.882	9.405	9.748	9.619	MKD
4249.78	8.719	9.211	9.573	9.603	MKD	4256.71	8.888	9.398	9.741	9.629	MKD
4249.82	8.729	9.223	9.571	9.608	MKD	4256.72	8.884	9.390	9.755	9.624	MKD
4249.83	8.720	9.211	9.561	9.594	MKD	4256.72	8.884	9.400	9.744	9.624	MKD
4249.84	8.756	9.233	9.563	9.606	MKD	4256.72	8.883	9.395	9.747	9.622	MKD
4250.71	8.714	9.209	9.569	9.598	MKD	4256.72	8.892	9.397	9.744	9.632	MKD
4250.71	8.701	9.226	9.588	9.612	MKD	4258.66	8.921	9.444	9.798	9.638	MKD
4250.72	8.732	9.220	9.588	9.602	MKD	4258.66	8.924	9.443	9.797	9.642	MKD
4250.75	8.690	9.203	9.559	9.583	MKD	4258.66	8.946	9.439	9.791	9.635	MKD
4250.75	8.698	9.209	9.565	9.586	MKD	4258.66	8.920	9.444	9.777	9.630	MKD
4250.76	8.730	9.225	9.573	9.606	MKD	4258.72	8.929	9.440	9.792	9.629	MKD
4250.76	8.734	9.221	9.581	9.615	MKD	4258.72	8.919	9.441	9.792	9.622	MKD
4250.77	8.706	9.207	9.558	9.577	MKD	4258.72	8.923	9.449	9.788	9.640	MKD
4250.77	8.709	9.217	9.566	9.599	MKD	4258.72	8.924	9.449	9.782	9.632	MKD
4250.77	8.725	9.214	9.561	9.589	MKD	4258.73	8.926	9.450	9.796	9.634	MKD
4250.77	8.717	9.207	9.569	9.591	MKD	4258.73	8.941	9.442	9.800	9.648	MKD
4253.68	8.815	9.305	9.669	9.637	MKD	4258.73	8.927	9.442	9.770	9.627	MKD
4253.68	8.815	9.305	9.671	9.623	MKD	4258.73	8.937	9.445	9.794	9.627	MKD
4253.69	8.821	9.309	9.677	9.632	MKD	4258.80	8.921	9.424	9.765	9.616	MKD
4253.69	8.820	9.315	9.668	9.637	MKD	4258.80	8.926	9.430	9.779	9.634	MKD
4253.72	8.799	9.310	9.678	9.639	MKD	4258.80	8.929	9.428	9.776	9.626	MKD
4253.72	8.803	9.311	9.668	9.640	MKD	4258.80	8.922	9.426	9.790	9.626	MKD
4253.73	8.806	9.299	9.660	9.641	MKD	4258.80	8.917	9.429	9.788	9.626	MKD
4253.73	8.798	9.303	9.666	9.640	MKD	4258.80	8.916	9.428	9.771	9.620	MKD
4253.73	8.810	9.301	9.659	9.645	MKD	4258.81	8.916	9.428	9.769	9.623	MKD
4253.73	8.816	9.309	9.667	9.647	MKD	4258.81	8.922	9.436	9.773	9.628	MKD
4253.74	8.819	9.296	9.665	9.636	MKD	4258.82	8.926	9.433	9.779	9.634	MKD
4253.74	8.811	9.303	9.664	9.647	MKD	4258.82	8.912	9.434	9.790	9.615	MKD
4253.75	8.817	9.299	9.647	9.635	MKD	4258.82	8.921	9.422	9.757	9.625	MKD
4253.79	8.817	9.302	9.648	9.636	MKD	4258.82	8.913	9.423	9.782	9.626	MKD
4253.80	8.811	9.313	9.660	9.635	MKD	4258.82	8.918	9.435	9.787	9.625	MKD
4253.80	8.814	9.301	9.659	9.639	MKD	4258.82	8.919	9.427	9.782	9.621	MKD
4253.80	8.799	9.298	9.659	9.634	MKD	4258.82	8.922	9.436	9.783	9.641	MKD
4253.80	8.793	9.291	9.659	9.635	MKD	4258.82	8.930	9.441	9.782	9.620	MKD
4253.81	8.795	9.306	9.643	9.626	MKD	4258.84	8.905	9.416	9.766	9.620	MKD
4253.81	8.788	9.299	9.649	9.620	MKD	4258.84	8.910	9.419	9.767	9.626	MKD
4253.81	8.807	9.297	9.654	9.630	MKD	4258.85	8.928	9.428	9.772	9.629	MKD
4253.81	8.795	9.298	9.656	9.635	MKD	4258.85	8.912	9.429	9.771	9.650	MKD
4253.82	8.807	9.303	9.659	9.631	MKD	4258.85	8.913	9.424	9.759	9.628	MKD
4253.83	8.798	9.299	9.651	9.632	MKD	4260.71	8.929	9.454	9.781	9.631	MKD
4253.83	8.793	9.304	9.648	9.624	MKD	4260.71	8.909	9.455	9.796	9.620	MKD
4253.84	8.793	9.296	9.655	9.628	MKD	4260.71	8.911	9.448	9.789	9.626	MKD
4253.84	8.789	9.306	9.659	9.617	MKD	4260.71	8.928	9.443	9.781	9.621	MKD
4254.65	8.818	9.322	9.675	9.607	MKD	4260.71	8.933	9.450	9.794	9.616	MKD
4254.65	8.810	9.320	9.675	9.603	MKD	4260.71	8.925	9.438	9.799	9.607	MKD
4254.65	8.817	9.317	9.675	9.601	MKD	4260.72	8.926	9.435	9.779	9.609	MKD
4254.66	8.821	9.313	9.666	9.584	MKD	4260.73	8.921	9.454	9.792	9.619	MKD
4254.72	8.846	9.347	9.690	9.628	MKD	4260.73	8.898	9.437	9.776	9.591	MKD
4254.72	8.843	9.357	9.695	9.632	MKD	4260.73	8.918	9.432	9.784	9.591	MKD
4254.72	8.846	9.353	9.697	9.637	MKD	4260.73	8.921	9.441	9.772	9.603	MKD
4254.72	8.837	9.353	9.702	9.641	MKD	4260.73	8.922	9.441	9.767	9.588	MKD
4254.73	8.844	9.350	9.713	9.632	MKD	4260.73	8.916	9.452	9.776	9.597	MKD
4254.73	8.844	9.352	9.722	9.638	MKD	4260.73	8.942	9.437	9.780	9.601	MKD
4254.73	8.843	9.337	9.722	9.642	MKD	4261.71	8.915	9.435	9.775	9.583	MKD
4254.73	8.852	9.345	9.726	9.644	MKD	4261.71	8.913	9.431	9.791	9.602	MKD
4254.74	8.851	9.352	9.719	9.642	MKD	4261.72	8.924	9.433	9.775	9.599	MKD
4254.74	8.841	9.360	9.727	9.642	MKD	4261.72	8.906	9.439	9.771	9.593	MKD
4254.77	8.854	9.355	9.696	9.662	MKD	4261.72	8.910	9.437	9.778	9.590	MKD
4254.77	8.850	9.357	9.706	9.665	MKD	4261.72	8.916	9.436	9.784	9.599	MKD
4254.77	8.856	9.360	9.704	9.660	MKD	4261.72	8.909	9.419	9.772	9.583	MKD
4254.77	8.864	9.357	9.697	9.662	MKD	4261.72	8.897	9.436	9.779	9.587	MKD
4254.80	8.846	9.358	9.715	9.663	MKD	4261.73	8.906	9.428	9.777	9.577	MKD
4254.80	8.859	9.355	9.711	9.654	MKD	4261.73	8.907	9.415	9.780	9.587	MKD
4254.80	8.860	9.360	9.713	9.648	MKD	4261.74	8.907	9.419	9.772	9.588	MKD
4254.80	8.873	9.368	9.719	9.655	MKD	4261.74	8.898	9.433	9.782	9.586	MKD
4254.80	8.863	9.354	9.737	9.653	MKD	4261.75	8.915	9.424	9.798	9.598	MKD
4254.81	8.862	9.363	9.730	9.659	MKD	4261.75	8.897	9.420	9.776	9.594	MKD
4254.81	8.867	9.360	9.728	9.658	MKD	4261.75	8.895	9.431	9.795	9.579	MKD
4254.81	8.872	9.366	9.716	9.649	MKD	4261.75	8.907	9.427	9.790	9.600	MKD
4254.81	8.870	9.375	9.714	9.654	MKD	4261.75	8.920	9.426	9.787	9.598	MKD
4255.65	8.813	9.321	9.683	9.555	MKD	4262.74	8.912	9.413	9.771	9.574	MKD
4255.65	8.831	9.328	9.692	9.559	MKD	4262.75	8.913	9.428	9.777	9.572	MKD
4255.65	8.815	9.311	9.679	9.562	MKD	4262.75	8.915	9.420	9.771	9.585	MKD
4255.66	8.798	9.320	9.691	9.558	MKD	4262.75	8.921	9.429	9.762	9.575	MKD
4255.66	8.822	9.335	9.695	9.564	MKD	4262.75	8.909	9.424	9.775	9.564	MKD
4255.66	8.823	9.342	9.700	9.567	MKD	4262.75	8.909	9.405	9.781	9.548	MKD
4255.71	8.819	9.326	9.666	9.573	MKD	4262.75	8.918	9.430	9.789	9.555	MKD
4255.71	8.814	9.331	9.664	9.578	MKD	4262.75	8.909	9.416	9.773	9.565	MKD
4255.71	8.805	9.326	9.673	9.572	MKD	4262.76	8.909	9.422	9.766	9.572	MKD
4255.71	8.813	9.324	9.671	9.574	MKD	4262.76	8.911	9.419	9.756	9.573	MKD
4255.71	8.820	9.326	9.668	9.583	MKD	4262.76	8.896	9.398	9.757	9.565	MKD
4255.71	8.816	9.332	9.679	9.570	MKD	4262.77	8.915	9.417	9.770	9.581	MKD
4255.73	8.818	9.326	9.681	9.574	MKD	4262.77	8.912	9.422	9.766	9.592	MKD
4255.73	8.819	9.331	9.677	9.566	MKD	4262.77	8.922	9.435	9.776	9.566	MKD
4255.73	8.812	9.329	9.676	9.571	MKD	4262.77	8.925	9.443	9.781	9.564	MKD
4255.73	8.830	9.334	9.679	9.568	MKD	4262.77	8.913	9.420	9.772	9.566	MKD
4255.73	8.814	9.326	9.686	9.571	MKD	4262.77	8.906	9.418	9.780	9.567	MKD
4255.81	8.817	9.334	9.696	9.557	MKD	4262.77	8.917	9.431	9.776	9.569	MKD
4255.81	8.831	9.333	9.683	9.560	MKD	4263.77	8.859	9.394	9.734	9.535	MKD
4255.82	8.830	9.324	9.699	9.564	MKD	4263.77	8.837	9.391	9.743	9.540	MKD
4255.82	8.832	9.333	9.686	9.549	MKD	4263.77	8.849	9.385	9.733	9.532	MKD
4255.82	8.834	9.320	9.694	9.555	MKD	4263.77	8.846	9.384	9.752	9.533	MKD

TABLE IIB *(continued)*.

JD. 2440000.+	Y	B	V	U	INSTRUMENT	JD. 2440000.+	Y	B	V	U	INSTRUMENT
4263.77	8.866	9.365	9.748	9.530	MKD	4275.79	8.537	9.043	9.360	9.552	KBO
4263.77	8.851	9.391	9.739	9.547	MKD	4275.79	8.539	9.034	9.373	9.546	KBO
4263.77	8.846	9.394	9.734	9.543	MKD	4275.80	8.542	9.043	9.346	9.534	KBO
4263.78	8.881	9.374	9.754	9.520	MKD	4275.80	8.529	9.032	9.349	9.544	KBO
4263.78	8.877	9.394	9.751	9.542	MKD	4276.66	8.546	9.049	9.408	9.541	KBO
4263.78	8.873	9.383	9.749	9.544	MKD	4276.66	8.537	9.073	9.412	9.540	KBO
4263.78	8.858	9.391	9.721	9.538	MKD	4276.72	8.557	9.074	9.409	9.547	KBO
4263.78	8.861	9.390	9.764	9.541	MKD	4276.72	8.556	9.070	9.410	9.550	KBO
4263.78	8.861	9.385	9.740	9.547	MKD	4276.73	8.566	9.071	9.410	9.557	KBO
4263.78	8.864	9.394	9.714	9.540	MKD	4276.73	8.575	9.061	9.396	9.556	KBO
4263.79	8.842	9.390	9.729	9.551	MKD	4276.74	8.572	9.074	9.424	9.558	KBO
4263.79	8.844	9.387	9.736	9.525	MKD	4276.74	8.559	9.087	9.418	9.565	KBO
4263.79	8.864	9.400	9.754	9.541	MKD	4276.75	8.580	9.096	9.426	9.564	KBO
4264.72	8.873	9.416	9.728	9.617	KBO	4276.75	8.580	9.097	9.432	9.572	KBO
4264.73	8.875	9.407	9.732	9.619	KBO	4276.76	8.589	9.097	9.425	9.577	KBO
4264.73	8.859	9.411	9.719	9.610	KBO	4276.81	8.582	9.117	9.428	9.586	KBO
4264.74	8.871	9.412	9.724	9.608	KBO	4276.82	8.599	9.106	9.432	9.580	KBO
4264.76	8.885	9.428	9.733	9.623	KBO	4276.82	8.585	9.108	9.448	9.588	KBO
4264.76	8.879	9.443	9.748	9.627	KBO	4276.82	8.589	9.107	9.418	9.589	KBO
4264.77	8.873	9.404	9.727	9.616	KBO	4277.66	8.553	9.066	9.377	9.541	KBO
4264.77	8.862	9.405	9.735	9.610	KBO	4277.66	8.558	9.069	9.379	9.535	KBO
4264.78	8.875	9.416	9.739	9.615	KBO	4277.78	8.526	9.048	9.388	9.528	KBO
4264.79	8.906	9.409	9.735	9.605	KBO	4277.78	8.537	9.058	9.384	9.517	KBO
4266.78	8.794	9.330	9.666	9.574	KBO	4277.79	8.538	9.055	9.382	9.523	KBO
4266.79	8.787	9.350	9.685	9.581	KBO	4277.79	8.532	9.045	9.385	9.527	KBO
4266.82	8.799	9.347	9.675	9.573	KBO	4277.80	8.542	9.063	9.376	9.539	KBO
4266.82	8.794	9.357	9.697	9.583	KBO	4277.80	8.531	9.048	9.395	9.539	KBO
4266.82	8.795	9.356	9.704	9.592	KBO	4277.81	8.544	9.059	9.386	9.533	KBO
4266.83	8.770	9.332	9.670	9.634	KBO	4277.81	8.543	9.066	9.393	9.528	KBO
4266.84	8.776	9.363	9.660	9.593	KBO	4277.82	8.547	9.074	9.396	9.531	KBO
4266.85	8.787	9.363	9.686	9.591	KBO	4277.82	8.551	9.075	9.382	9.534	KBO
4268.72	8.697	9.262	9.574	9.557	KBO	4277.83	8.533	9.064	9.399	9.534	KBO
4268.72	8.703	9.255	9.562	9.559	KBO	4277.84	8.552	9.070	9.405	9.540	KBO
4268.73	8.702	9.262	9.594	9.557	KBO	4278.66	8.697	9.210	9.534	9.681	KBO
4268.73	8.703	9.266	9.596	9.568	KBO	4278.66	8.699	9.211	9.539	9.677	KBO
4268.74	8.709	9.259	9.590	9.566	KBO	4278.73	8.663	9.193	9.532	9.671	KBO
4268.74	8.709	9.246	9.574	9.565	KBO	4278.73	8.690	9.218	9.547	9.667	KBO
4268.75	8.709	9.242	9.564	9.563	KBO	4278.77	8.678	9.192	9.513	9.661	KBO
4268.75	8.702	9.237	9.574	9.561	KBO	4278.78	8.687	9.207	9.529	9.665	KBO
4268.78	8.698	9.259	9.590	9.560	KBO	4278.79	8.673	9.190	9.526	9.661	KBO
4268.79	8.688	9.254	9.572	9.554	KBO	4278.82	8.660	9.189	9.528	9.662	KBO
4268.80	8.710	9.267	9.573	9.554	KBO	4279.66	8.703	9.211	9.567	9.673	KBO
4268.80	8.703	9.254	9.589	9.554	KBO	4279.66	8.709	9.228	9.586	9.680	KBO
4268.81	8.706	9.252	9.562	9.555	KBO	4279.72	8.709	9.251	9.578	9.685	KBO
4268.82	8.714	9.256	9.561	9.561	KBO	4279.72	8.712	9.253	9.585	9.685	KBO
4268.82	8.693	9.256	9.567	9.541	KBO	4279.73	8.706	9.241	9.595	9.684	KBO
4268.82	8.698	9.251	9.572	9.540	KBO	4279.73	8.708	9.247	9.601	9.683	KBO
4269.71	8.656	9.209	9.549	9.521	KBO	4279.73	8.707	9.238	9.579	9.690	KBO
4269.71	8.668	9.195	9.548	9.512	KBO	4279.74	8.709	9.228	9.589	9.690	KBO
4269.72	8.657	9.214	9.530	9.518	KBO	4279.74	8.703	9.236	9.592	9.688	KBO
4269.72	8.647	9.207	9.539	9.521	KBO	4279.75	8.701	9.250	9.577	9.689	KBO
4269.73	8.655	9.212	9.528	9.532	KBO	4279.75	8.705	9.236	9.579	9.686	KBO
4269.73	8.649	9.211	9.539	9.529	KBO	4279.76	8.720	9.243	9.588	9.687	KBO
4269.74	8.653	9.205	9.545	9.529	KBO	4280.72	8.725	9.260	9.577	9.695	KBO
4269.74	8.665	9.212	9.543	9.531	KBO	4280.72	8.745	9.263	9.584	9.698	KBO
4269.80	8.633	9.183	9.510	9.514	KBO	4280.73	8.741	9.260	9.581	9.686	KBO
4269.80	8.655	9.190	9.517	9.513	KBO	4280.73	8.731	9.286	9.592	9.688	KBO
4269.80	8.634	9.195	9.518	9.511	KBO	4280.80	8.730	9.264	9.600	9.671	KBO
4270.76	8.630	9.168	9.464	9.549	KBO	4280.81	8.724	9.262	9.573	9.671	KBO
4270.76	8.627	9.162	9.462	9.542	KBO	4280.82	8.719	9.264	9.581	9.669	KBO
4271.72	8.534	9.051	9.372	9.467	KBO	4280.82	8.716	9.294	9.615	9.677	KBO
4271.72	8.533	9.058	9.392	9.457	KBO	4280.82	8.728	9.290	9.600	9.681	KBO
4271.73	8.533	9.059	9.406	9.455	KBO	4280.83	8.722	9.283	9.571	9.680	KBO
4271.73	8.534	9.064	9.395	9.456	KBO	4280.84	8.743	9.267	9.590	9.688	KBO
4271.73	8.543	9.059	9.385	9.454	KBO	4282.65	8.780	9.288	9.641	9.676	KBO
4271.74	8.543	9.069	9.380	9.460	KBO	4282.65	8.777	9.297	9.638	9.679	KBO
4271.75	8.554	9.070	9.391	9.451	KBO	4282.66	8.772	9.293	9.626	9.687	KBO
4271.75	8.554	9.063	9.383	9.452	KBO	4282.66	8.775	9.301	9.627	9.670	KBO
4271.76	8.553	9.074	9.385	9.455	KBO	4282.75	8.773	9.305	9.650	9.681	KBO
4271.77	8.558	9.066	9.375	9.453	KBO	4282.75	8.762	9.302	9.639	9.674	KBO
4271.78	8.520	9.069	9.391	9.454	KBO	4282.75	8.762	9.282	9.634	9.676	KBO
4271.79	8.549	9.064	9.405	9.454	KBO	4282.75	8.769	9.306	9.619	9.682	KBO
4272.74	8.559	9.031	9.368	9.451	KBO	4282.76	8.771	9.293	9.612	9.676	KBO
4272.74	8.555	9.024	9.374	9.453	KBO	4282.77	8.769	9.298	9.630	9.684	KBO
4272.75	8.559	9.036	9.363	9.459	KBO	4282.77	8.768	9.312	9.621	9.683	KBO
4272.75	8.565	9.038	9.344	9.457	KBO	4282.78	8.773	9.291	9.601	9.680	KBO
4272.76	8.553	9.039	9.350	9.455	KBO	4282.78	8.759	9.309	9.625	9.682	KBO
4272.77	8.553	9.047	9.365	9.463	KBO	4283.66	8.793	9.319	9.617	9.680	KBO
4272.78	8.553	9.035	9.321	9.462	KBO	4283.66	8.792	9.321	9.623	9.680	KBO
4272.79	8.536	9.022	9.329	9.462	KBO	4283.66	8.776	9.296	9.616	9.679	KBO
4272.79	8.545	9.029	9.330	9.462	KBO	4283.66	8.795	9.307	9.634	9.682	KBO
4273.69	8.579	9.078	9.426	9.576	KBO	4283.77	8.739	9.279	9.571	9.642	KBO
4273.70	8.585	9.066	9.433	9.582	KBO	4283.78	8.745	9.265	9.586	9.643	KBO
4273.70	8.583	9.086	9.416	9.576	KBO	4283.79	8.748	9.260	9.563	9.646	KBO
4273.71	8.579	9.069	9.411	9.583	KBO	4283.79	8.747	9.261	9.558	9.639	KBO
4273.71	8.584	9.078	9.403	9.584	KBO	4283.79	8.777	9.265	9.583	9.639	KBO
4273.72	8.588	9.082	9.416	9.582	KBO	4284.74	8.859	9.387	9.719	9.699	KBO
4273.72	8.585	9.068	9.415	9.580	KBO	4284.75	8.859	9.372	9.708	9.694	KBO
4273.74	8.588	9.072	9.414	9.576	KBO	4284.76	8.863	9.394	9.707	9.700	KBO
4273.75	8.593	9.090	9.424	9.587	KBO	4284.76	8.858	9.383	9.710	9.701	KBO
4273.75	8.591	9.085	9.417	9.584	KBO	4284.77	8.842	9.392	9.724	9.711	KBO
4273.76	8.588	9.101	9.416	9.585	KBO	4284.77	8.867	9.381	9.710	9.689	KBO
4273.77	8.592	9.102	9.427	9.597	KBO	4284.77	8.855	9.376	9.714	9.704	KBO
4273.77	8.589	9.087	9.424	9.594	KBO	4213.85	8.846	9.337	9.705	9.701	ARD
4273.79	8.592	9.111	9.411	9.600	KBO	4214.84	8.811	9.346	9.693	9.640	ARD
4273.79	8.585	9.108	9.420	9.604	KBO	4217.84	8.924	9.434	9.772	9.672	ARD
4273.80	8.586	9.109	9.419	9.602	KBO	4218.84	9.045	9.550	9.883	9.754	ARD
4273.80	8.588	9.110	9.442	9.605	KBO	4219.84	9.067	9.578	9.904	9.772	ARD
4273.81	8.592	9.101	9.440	9.607	KBO	4223.84	9.108	9.616	9.955	9.824	ARD
4273.81	8.598	9.113	9.444	9.618	KBO	4226.84	9.080	9.595	9.940	9.790	ARD
4273.82	8.589	9.108	9.447	9.615	KBO	4227.84	9.056	9.578	9.914	9.789	ARD
4273.82	8.608	9.100	9.445	9.626	KBO	4228.84	9.085	9.600	9.944	9.813	ARD
4274.73	8.483	8.967	9.277	9.481	KBO	4229.85	9.038	9.581	9.905	9.770	ARD
4274.73	8.480	8.965	9.290	9.468	KBO	4230.84	9.046	9.557	9.901	9.770	ARD
4274.73	8.486	8.962	9.276	9.475	KBO	4231.84	8.971	9.476	9.799	9.679	ARD
4274.73	8.486	8.963	9.277	9.466	KBO	4232.84	8.960	9.469	9.817	9.696	ARD
4275.76	8.551	9.045	9.361	9.553	KBO	4233.85	8.907	9.420	9.766	9.682	ARD
4275.77	8.540	9.047	9.366	9.550	KBO	4234.85	8.825	9.336	9.694	9.604	ARD
4275.77	8.557	9.031	9.356	9.544	KBO	4235.84	8.774	9.300	9.644	9.571	ARD
4275.77	8.536	9.042	9.358	9.543	KBO	4236.84	8.688	9.200	9.559	9.553	ARD
4275.78	8.545	9.036	9.355	9.550	KBO	4237.85	8.686	9.187	9.525	9.513	ARD
4275.78	8.532	9.028	9.353	9.549	KBO	4239.84	8.632	9.140	9.483	9.497	ARD

TABLE IIB *(continued).*

JD. 2440000.+	Y	B	V	U	INSTRUMENT
4240.84	8.655	9.146	9.482	9.558	ARD
4241.84	8.565	9.059	9.402	9.502	ARD
4242.84	8.554	9.026	9.362	9.461	ARD
4243.84	8.569	9.056	9.398	9.519	ARD
4247.82	8.632	9.116	9.448	9.518	ARD
4248.75	8.710	9.194	9.526	9.600	ARD
4264.85	8.849	9.386	9.736	9.542	ARD
4265.86	8.801	9.352	9.699	9.526	ARD
4266.86	8.762	9.313	9.686	9.516	ARD
4268.85	8.696	9.221	9.593	9.506	ARD
4271.84	8.540	9.029	9.396	9.400	ARD
4272.79	8.537	9.013	9.360	9.402	ARD
4273.82	8.602	9.080	9.448	9.558	ARD
4274.79	8.483	8.956	9.320	9.427	ARD
4275.82	8.525	8.994	9.359	9.466	ARD
4276.81	8.573	9.077	9.455	9.543	ARD
4277.79	8.537	9.027	9.398	9.480	ARD
4278.70	8.691	9.181	9.552	9.630	ARD
4359.61	8.702	9.198	9.558	9.611	ARD
4359.62	8.693	9.199	9.553	9.609	ARD
4360.57	8.677	9.185	9.560	9.566	ARD
4361.65	8.595	9.101	9.476	9.523	ARD
4362.49	8.668	9.158	9.521	9.601	ARD
4406.45	8.848	9.342	9.695	9.676	ARD
4406.46	8.846	9.343	9.695	9.670	ARD
4407.52	8.883	9.375	9.725	9.677	ARD
4407.53	8.882	9.379	9.724	9.675	ARD
4408.46	8.942	9.454	9.790	9.786	ARD
4412.55	8.933	9.433	9.773	9.651	ARD
4416.47	8.827	9.297	9.656	9.741	ARD
4416.49	8.824	9.295	9.656	9.732	ARD
4417.49	8.747	9.240	9.590	9.622	ARD
4417.50	8.748	9.237	9.592	9.611	ARD
4423.49	8.622	9.119	9.474	9.540	ARD
4431.50	8.538	8.982	9.347	9.475	ARD
4432.50	8.630	9.056	9.415	9.540	ARD
4442.46	8.890	9.395	9.735	9.756	ARD
4451.48	8.593	9.066	9.401	9.466	ARD
4451.50	8.583	9.058	9.396	9.465	ARD
4456.52	8.530	8.974	9.317	9.667	ARD
4456.52	8.527	8.968	9.314	9.657	ARD
4457.48	8.577	9.055	9.402	9.670	ARD
4457.49	8.267	8.740	9.096	9.351	ARD
4458.47	8.514	8.970	9.318	9.532	ARD
4459.47	8.543	8.994	9.343	9.627	ARD
4460.47	8.627	9.106	9.462	9.662	ARD
4461.47	8.485	8.950	9.304	9.509	ARD
4462.48	8.550	8.996	9.349	9.554	ARD
4462.50	8.550	9.001	9.351	9.551	ARD
4464.49	8.586	9.040	9.378	9.495	ARD
4464.50	8.588	9.049	9.385	9.489	ARD
4468.48	8.840	9.339	9.692	9.665	ARD
4468.50	8.838	9.342	9.691	9.657	ARD
4469.48	8.769	9.250	9.600	9.576	ARD
4470.48	8.851	9.333	9.684	9.663	ARD
4474.49	8.848	9.333	9.676	9.645	ARD
4546.84	8.553	9.044	9.420	9.606	ARD
4546.85	8.547	9.048	9.418	9.610	ARD
4561.81	8.961	9.487	9.837	9.766	ARD
4561.82	8.960	9.486	9.841	9.777	ARD
4565.82	8.919	9.430	9.780	9.705	ARD
4565.83	8.919	9.431	9.780	9.705	ARD
4566.81	8.970	9.485	9.836	9.778	ARD
4566.82	8.976	9.490	9.841	9.779	ARD
4567.81	8.959	9.484	9.836	9.782	ARD
4567.82	8.963	9.477	9.841	9.794	ARD
4568.81	8.945	9.457	9.805	9.789	ARD
4568.82	8.942	9.453	9.807	9.788	ARD
4569.81	8.977	9.505	9.866	9.823	ARD
4569.82	8.978	9.505	9.862	9.830	ARD
4570.81	8.960	9.488	9.847	9.775	ARD
4570.82	8.964	9.487	9.849	9.782	ARD
4571.81	8.933	9.460	9.819	9.771	ARD
4571.82	8.931	9.460	9.820	9.771	ARD
4572.82	8.917	9.455	9.816	9.786	ARD
4572.83	8.915	9.451	9.819	9.790	ARD
4573.81	8.881	9.405	9.764	9.687	ARD
4573.82	8.881	9.415	9.771	9.698	ARD
4574.82	8.850	9.389	9.760	9.674	ARD
4574.83	8.850	9.383	9.755	9.670	ARD
4577.81	8.611	9.146	9.519	9.521	ARD
4577.82	8.608	9.149	9.522	9.525	ARD
4616.78	8.590	9.079	9.446	9.528	ARD
4616.79	8.602	9.073	9.447	9.533	ARD
4617.80	8.586	9.060	9.407	9.523	ARD
3886.77	8.987	9.502	9.842	9.725	JPS
3887.75	8.998	9.534	9.873	9.809	JPS
3888.77	8.958	9.503	9.849	9.759	JPS
3890.75	8.845	9.352	9.691	9.657	JPS
3892.77	8.815	9.318	9.645	9.672	JPS
3893.78	8.769	9.273	9.606	9.600	JPS
3894.71	8.700	9.219	9.558	9.541	JPS
3895.71	8.699	9.220	9.560	9.541	JPS
3914.78	8.969	9.507	9.862	9.859	JPS
3915.73	8.876	9.422	9.791	9.904	JPS

KEY TO SYMBOLS : MKD DANISH 50 CM.(1980)
KBO BOCHUM 61 CM.(1980)
ARD ARDEBERG'S DATA (1979-80-81)
JPS BOCHUM 61 CM.(1979)

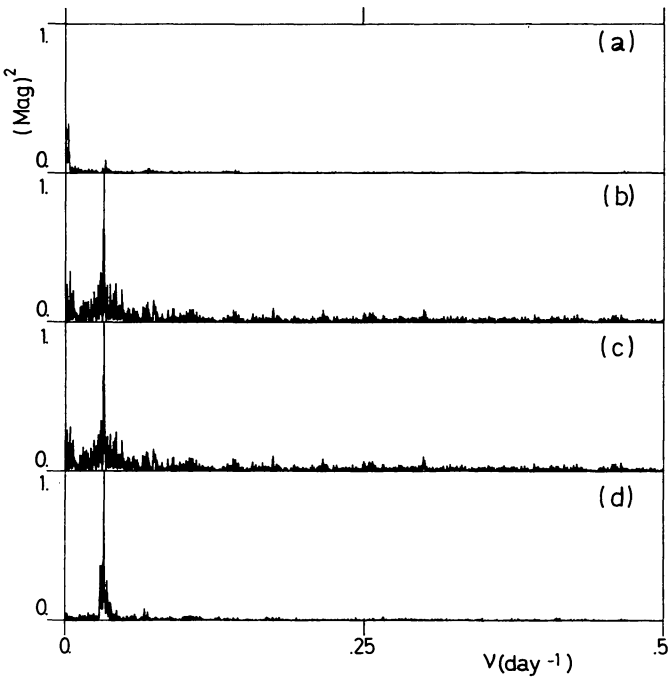

FIGURE 1. — Fourier analysis of photographic data as observed by Kruytbosch (1930) for GG Carinae. (a) square of the full amplitude of the spectral window (as defined by Deeming (1975)) ; (b) square of the full amplitude of the DFT (as also defined by Deeming (1975)) ; (c) spectral estimate P (ν) for the data (as defined by Ponman (1982)) ; (d) spectral estimate for a pure sine monochromatic wave (see text).

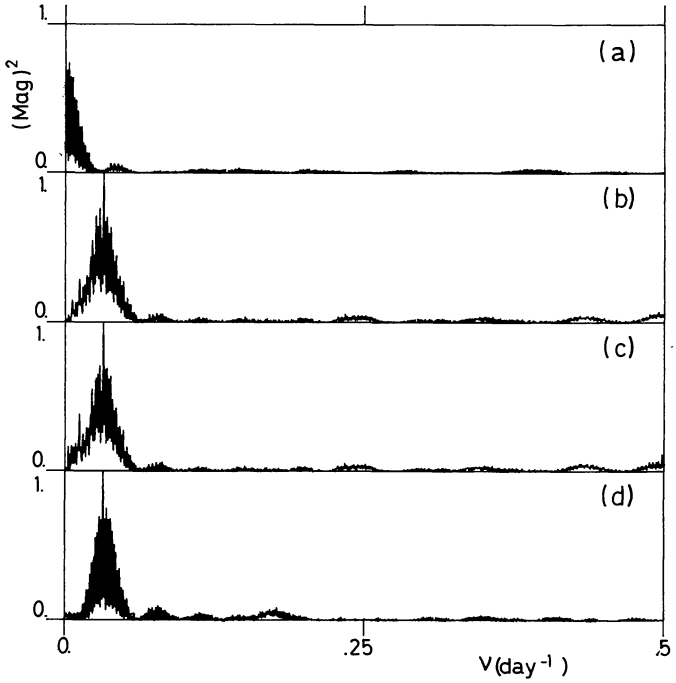

FIGURE 2. — Fourier analysis of the photometric data listed in table II. The four parts are essentially defined as in figure 1 (see text).

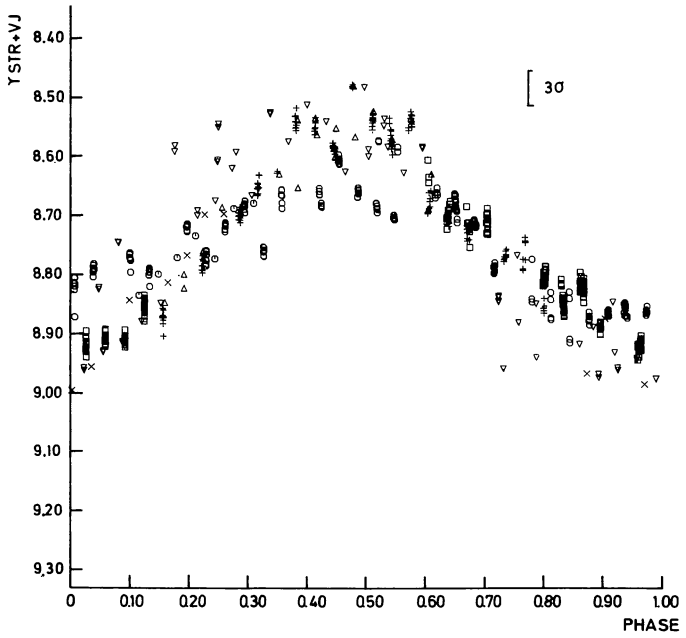

FIGURE 3. — Composite lightcurve for GG Carinae adopting a period of 31.020 days. The epoch of the minimum (ϕ = 0) is from table III. The symbols are related to initials in table II : □ = y mag in MKD ; + = y mag in KBO ; △ = y mag from ARD before March, 1980 ; ▽ = y mag from ARD after March, 1980 ; × = y mag from JPS ; ○ = V mag in the UBV set ; ○ = V mag in the UXV set.

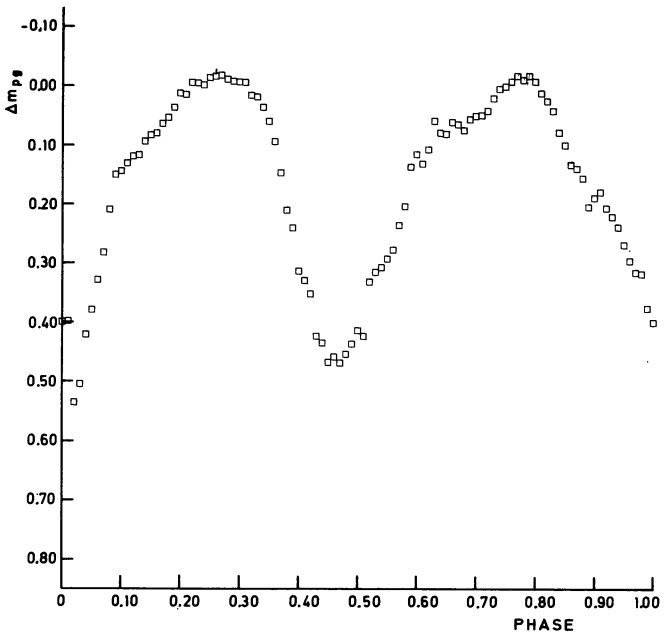

FIGURE 5. — Sliding (unweighted) mean through a phase diagram constructed from Kruytbosch's data adopting a period of 62.102 days (≡ 2 × 31.051). The epoch of the minimum is that derived by Kruytbosch (1930). The abscissae give the phase and the ordinates represent relative photographic magnitudes as published by Kruytbosch.

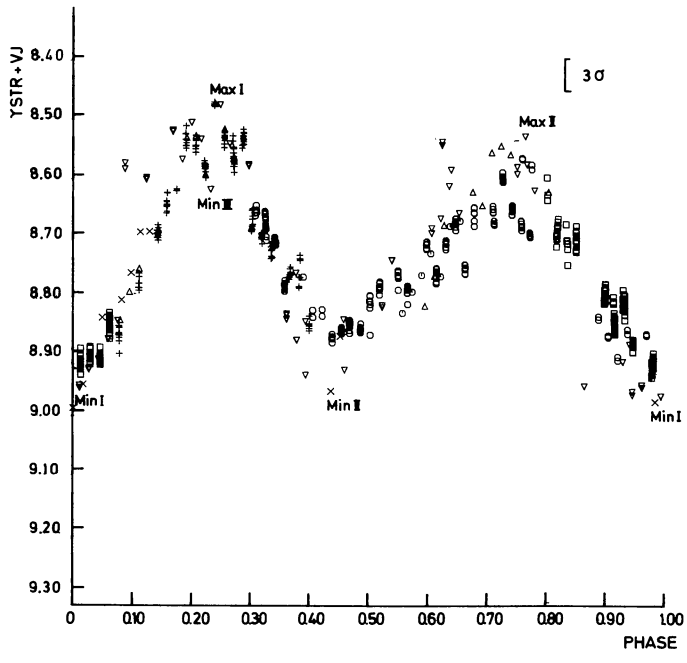

FIGURE 4. — Same as for Fig. 3 with P = 62.039 days.

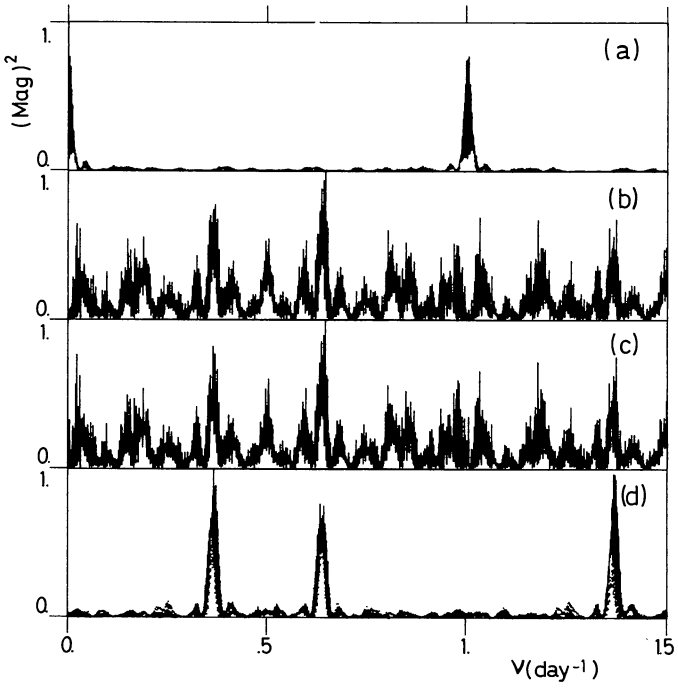

FIGURE 6. — Fourier analysis of our y and V data whitened for the main variation (see text). Parts a, b, c are as for Figs. 1 and 2. In part d, the spectral estimates for two pure sine monochromatic waves are given. These were sampled in exactly the same way as were our data. The continuous (resp. dotted) line is for a frequency ν = 0.3657 day^{-1} (resp. 0.6356 day^{-1}) of the sine wave.

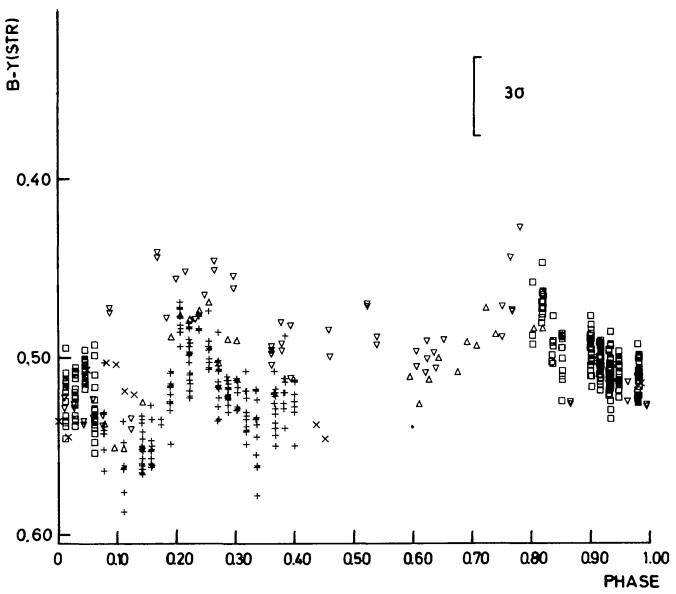

FIGURE 7. — Variation of the *b-y* color adopting a 62.039 day period. The symbols are the same as those in Fig. 3 (the *UBV* photometry being deleted here).

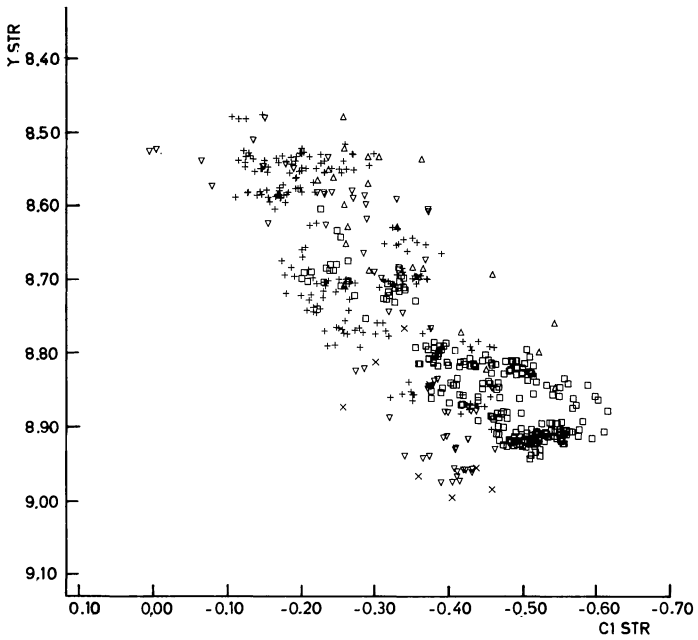

FIGURE 8. — Correlation between the *y* mag and the c_1 index in the Strömgren system.